Chapter 7

Using RNA Nanoparticles with Thermostable Motifs and Fluorogenic Modules for Real-Time Detection of RNA Folding and Turnover In Prokaryotic and Eukaryotic Cells

Hui Zhang, Fengmei Pi, Dan Shu, Mario Vieweger, and Peixuan Guo

Abstract

RNA nanotechnology is an emerging field at the interface of biochemistry and nanomaterials that shows immense promise for applications in nanomedicines, therapeutics and nanotechnology. Noncoding RNAs, such as siRNA, miRNA, ribozymes, and riboswitches, play important roles in the regulation of cellular processes. They carry out highly specific functions on a compact and efficient footprint. The properties of specificity and small size make them excellent modules in the construction of multifaceted RNA nanoparticles for targeted delivery and therapy. Biological activity of RNA molecules, however, relies on their proper folding. Therefore their thermodynamic and biochemical stability in the cellular environment is critical. Consequently, it is essential to assess global fold and intracellular lifetime of multifaceted RNA nanoparticles to optimize their therapeutic effectiveness. Here, we describe a method to express and assemble stable RNA nanoparticles in cells, and to assess the folding and turnover rate of RNA nanoparticles in vitro as well as in vivo in real time using a thermostable core motif derived from pRNA of bacteriophage Phi29 DNA packaging motor and fluorogenic RNA modules.

Key words pRNA-3WJ, RNA nanotechnology, In vivo imaging, Aptamer, Fluorogenic RNA

1 Introduction

RNA nanotechnology has received increasing attention in recent years due to its versatility and breath of applications in nanomaterials and therapeutics [1–6]. It makes use of the inherent biochemical activity of noncoding RNA elements in the construction of multifaceted nanoparticles with application-specific programmable designs. The increasing discovery of novel noncoding RNA elements clearly illustrates the diversity and importance of structural RNA in the regulation of cellular functions [7–10]. These functions, e.g., receptor binding and enzymatic catalysis, are desirable characteristics for specific targeting and directed activity of therapeutic nanoparticles. RNA nanotechnology makes use of this intrinsic functionality by incorporating particular structural RNA

Peixuan Guo and Farzin Haque (eds.), *RNA Nanotechnology and Therapeutics: Methods and Protocols*,
Methods in Molecular Biology, vol. 1297, DOI 10.1007/978-1-4939-2562-9_7,

motifs as modules in RNA nanoparticles [3, 11, 12]. For ease of adaptability these modules are typically fused to a structural core that builds the scaffold of the nanoparticle construct featuring specific sites for attachment of the modules. This structural core therefore plays a major role in the overall global fold, thermodynamic stability and intracellular degradation of the nanoparticle, while the modular RNA motifs determine the application-specific properties.

Successful application of RNA nanoparticles in nanomedicine and therapeutics requires that activity of the functional modules is retained after fusion to the core scaffold. Activity of the RNA module depends on proper global folding of its tertiary structure, isolation from intramolecular interaction between functional modules, and accessibility required for execution of its function, e.g., binding of a receptor molecule. To a large extent, these parameters are controlled by the selection of the nanoparticle scaffold. A core structure with inherent structural features providing defined spatial separation of the modules, as in the 3WJ motif of the phi29 pRNA, significantly enhances the prospect of RNA activity. Although the overall secondary structure of the RNA nanoparticle can be predicted through several available RNA folding programs, prediction of the global RNA tertiary structure is still challenging. Therefore, evaluation of individual 3D RNA nanoparticle structures is essential for effective application.

Another consideration in RNA nanotechnology-based therapy is the in vivo stability of RNA, both in body and in cells. Since RNA is detected and removed through cellular defense mechanisms including innate immunity system such as Toll like receptors and nuclease digestion, its lifetime is typically rather limited. Chemical modification of RNA for example to 2′F-RNA can severely improve the stability against nuclease digestion in vivo. Nonetheless, RNA nanoparticles may still misfold or be degraded in the cells, resulting in loss of RNA activity. Determination of the intracellular half-life of the modular nanoparticle, its overall structure and RNA activity is therefore vital in optimization of its therapeutic effect. Here we describe simple but effective approaches to construct stable and functional RNA nanoparticles expressed and assembled in cells, and to determine their intracellular turnover, folding and activity, using fluorogenic RNA aptamer modules fused to the thermostable 3WJ core motif.

Recent studies have demonstrated that the three-way junction (3WJ) core of phi29 motor RNA is thermodynamically stable [11] and drives folding of the entire RNA molecule [13]. It further provides three specific sites for fusion of RNA modules providing well-defined spatial separation and multi-functionality of RNA 3WJ-core nanoparticles; an ideal platform for the design of modular RNA nanoparticles. Fluorogenic RNA modules, such as Malachite Green (MG) [14] or Spinach [15] RNA aptamer, serve as detection modules to assess the global fold of the RNA

nanoparticle and monitor its degradation in cells, when fused to the RNA nanoparticles [11, 13, 15–24]. These RNA aptamers are not inherently fluorescent, but rather enhance the emission of weakly fluorescent dyes through stabilization of their emissive conformation upon binding. Due to the high specificity and affinity of the aptamer–reporter dye interaction, misfolding of the RNA nanoparticle leads to loss of binding capability and thus reduction of fluorescence intensity. This property allows real-time monitoring of RNA folding and degradation.

Following are detailed methods for the design and expression of fluorogenic RNA nanoparticles, as well as protocols to determine their activity and lifetime in vitro and in vivo. Initially, the design of modular RNA nanoparticles (Subheading 3.1) is outlined, as well as routes for their preparation in vitro (Subheading 3.2) and in vivo in bacterial cells (Subheading 3.3). Next, in vitro assessment of RNA folding and activity is discussed using native polyacrylamide gel electrophoresis (Subheading 3.4), MG binding assay (Subheading 3.5), and DHBFI binding assay (Subheading 3.6). Furthermore, a procedure to monitor misfolding and degradation of RNA nanoparticles in vitro is outlined (Subheading 3.7). Protocols for RNA activity in vivo are explained for bacterial cells (Subheading 3.8) and eukaryotic cells (Subheading 3.9). Finally, determination of the turnover of RNA nanoparticles in vivo is explained via determination of the degradation half-life in living cells (Subheading 3.10).

2 Materials

Prepare all solutions using Milli-Q water (18 mΩ cm at 25 °C). Store all solutions at room temperature unless otherwise indicated.

2.1 In Vitro Transcription and Purification of RNA

1. DEPC-treated water: 0.05 % (vol/vol) DEPC, Milli-Q water. Add 0.05 mL diethyl pyrocarbonate (DEPC) to 99.95 mL of Milli-Q water, shake vigorously, and incubate at 37 °C overnight. Autoclave to sterilize and remove the DEPC.
2. GoTaq flexi DNA polymerase (Promega, Madison, WI).
3. Transcription buffer (5×): 400 mM HEPES (pH 7.5), 120 mM magnesium chloride, 10 mM spermidine, and 200 mM dithiothreitol (DTT). Filtrate with a 0.22-μm syringe filter and store aliquots at −20 °C.
4. rNTP solution (25 mM): 25 mM ATP, 25 mM UTP, 25 mM GTP, 25 mM CTP (Life Technologies, Grand Island, NY) in DEPC-treated water.
5. T7 RNA polymerase: expressed in-house or acquired commercially.
6. RNase-free DNase I: 1 U/μL (Thermo Scientific, Waltham, MA).

7. TBE buffer (1×): 89 mM Tris base, 89 mM boric acid, and 2 mM EDTA (ethylenediaminetetraacetic acid).
8. Polyacrylamide gel running equipment (Thermo Scientific, Waltham, MA).
9. Denaturing loading buffer (2×): 95 % (vol/vol) formamide, 18 mM EDTA, 0.025 % (wt/vol) SDS, 0.025 % (wt/vol) bromophenol blue, and 0.025 % (wt/vol) xylene cyanol.
10. Denaturing PAGE gel (8 %): 8 % (wt/vol) polyacrylamide, 8 M urea, 1× TBE buffer. Dissolve 7.6 % (wt/vol) acrylamide, 0.4 % (wt/vol) *N,N*-methylenebisacrylamide, and 8 M urea in 1× TBE buffer to prepare an 8 % acrylamide–urea stock solution. To obtain a 5 mL polyacrylamide gel, add 50 μL 10 % (wt/vol) ammonium persulfate (APS) in Milli-Q water and 5 μL *N,N,N,N′*-tetramethyl-ethylenediamine (TEMED) to 5 mL of the acrylamide–urea stock solution.
11. TLC plates (Thermo Scientific, Waltham, MA).
12. UVGL-25 short wave (254 nm) UV lamp (UVP, Upland, CA).
13. RNA elution buffer: 0.5 M ammonium acetate, 0.1 mM EDTA, and 0.1 % (wt/vol) SDS in DEPC treated water.
14. TB buffer (1×): 89 mM Tris base, 200 mM boric acid, pH 7.8.
15. TBM buffer (1×): 89 mM Tris base, 200 mM boric acid, 5 mM magnesium chloride, pH 7.8.
16. Native loading buffer (6×): 0.025 % (wt/vol) bromophenol blue, 0.025 % (wt/vol) xylene cyanol, 40 % (wt/vol) sucrose.
17. Native Polyacrylamide gel (8 %): 8 % (wt/vol) polyacrylamide, 1× TBM buffer. To prepare 5 mL polyacrylamide gel, mix 8 % (wt/vol) (29:1) acrylamide–bis-acrylamide solution with 1× Tris–borate buffer (pH 7.8) and 5 mM magnesium chloride to a total volume of 5 mL, and add 50 μL 10 % (wt/vol) APS and 6 μL TEMED.
18. Savant DNA120 SpeedVac Concentrator (Thermo Scientific, Waltham, MA), or equivalent.
19. NanoDrop 2000 Spectrophotometer (Thermo Scientific, Waltham, MA), or equivalent.

2.2 Expression of RNA in E. coli.

1. Mini-sub cell GT agarose gel electrophoresis system (Bio-Rad, Hercules, CA), or equivalent.
2. QIAEXII gel extraction kit (Qiagen, Valencia, CA), or equivalent.
3. BglII and NdeI restriction enzymes and 10× fast digest buffer (Thermo Scientific, Waltham, MA).
4. T4 DNA ligase and 10× T4 DNA ligase buffer (New England Biolabs, Ipswitch, MA).

5. AxyPrep™ DNA gel extraction kit (Axygen Biosciences, Union City, CA), or equivalent.
6. LB medium: 1 % (wt/vol) tryptone, 0.5 % (wt/vol) yeast extract, 1 % (wt/vol) sodium chloride. Dissolve 10 g tryptone, 5 g yeast extract, and 10 g sodium chloride and bring the final volume to 1 L with Milli-Q water. Autoclave and store at 4 °C until use.
7. LB medium containing ampicillin: 1× LB medium, 100 μg/mL ampicillin.
8. IPTG solution: 1 M Isopropyl β-D-1-thiogalactopyranoside (IPTG).
9. Tris–HCl–Mg buffer: 1 mM Tris–HCl, 10 mM magnesium chloride, pH 7.4.
10. Water-saturated phenol (pH 4.5) (Thermo Scientific, Waltham, MA).
11. TSS buffer: 10 % (wt/vol) polyethylene glycol 8000 (PEG-8000), 5 % (vol/vol) dimethyl sulfoxide (DMSO), 20 mM magnesium chloride in LB medium. Mix 0.5 g PEG-8000, 0.25 mL DMSO, and 0.1 mL of 1 M magnesium chloride, and bring the final volume to 5 mL with autoclaved LB medium. Vortex thoroughly and filtrate through a 0.22 μm syringe filter. Store at −20 °C.
12. Competent *E. coli*. BL21 star cells: inoculate cells from an overnight culture at 1:50 with LB medium and grow until OD_{600} reaches 0.5–0.6. Chill the cells on ice and spin 1 mL cells down in a 1.6 mL sterile eppendorf tube at 4 °C for 2 min at 845 × *g*. Discard the supernatant and gently resuspend the cells in 100 μL of ice-cold TSS buffer. The competent cells can be used directly or immediately frozen on dry ice and then stored at −80 °C.
13. KCM buffer (5×): 500 mM potassium chloride, 150 mM calcium chloride, 250 mM magnesium chloride in Milli-Q water. Vortex thoroughly and filtrate through a 0.22 μm syringe filter. Store at −20 °C.

2.3 In Vitro and In Vivo MG/DFHBI Binding Assays

1. MG stock solution (for MG aptamer): 1 mM malachite green oxalate (MG) (Sigma-Aldrich, St. Louis, MO). Prepare stock solution in DEPC water and protect from light. Store at −20 °C.
2. DFHBI stock solution (for Spinach aptamer): 1 mM 3,5-difluoro-4-hydroxybenzylidene imidazolinone (DFHBI) (Lucerna Inc., New York, NY). Prepare stock solution in DEPC water and protect from light. Store at −20 °C.
3. Binding buffer (1×): 100 mM potassium chloride, 5 mM magnesium chloride and 10 mM HEPES, pH 7.4.

4. Typhoon FLA 7000 gel imager (GE Healthcare, Fairfield, CT), or equivalent.
5. FluoroLog Spectrofluorometer (Horiba Jobin Yvon, Edison, NJ), or equivalent.
6. Phosphate Buffered Saline (PBS): 137 mM sodium chloride, 2.7 mM potassium chloride, 10 mM sodium phosphate dibasic, and 2 mM potassium phosphate monobasic, pH 7.4.
7. PBS with magnesium: 1× PBS, 10 mM magnesium chloride, pH 7.4.
8. KB cell line: Human nasopharyngeal carcinoma KB cells (American Type Culture Collection, Manassas, VA).
9. RPMI1640 cell culture medium (Life Technologies, Grand Island, NY).
10. KB cell culture medium: Gibco® RPMI 1640 medium, 10 % (vol/vol) fetal bovine serum (FBS, Sigma Chemical Company, St. Louis, MO).
11. KB cell lysate: KB cells treated with Radio-Immuno Precipitation Assay (RIPA) lysis buffer.
12. Gene pulser (Bio-Rad, Hercules, CA), or equivalent.

2.4 Fluorescence Imaging of RNA Expression, Folding and Degradation in Animal and Human Cells

1. Inverted epi-fluorescence microscope: Olympus IX71, Halogen lamp, Xenon arc lamp, CCD camera (Olympus, Center Valley, PA), or equivalent.
2. MG compatible filter set: Cy5 filter cube with ET620/60 excitation filter, ET700/75 emission filter and T660lpxr dichroic (Chroma Technology Corp. Bellows Falls, VT.), or equivalent.
3. DFHBI compatible filter set: GFP filter cube with ET470/40 excitation filter, ET525/50 emission filter and T495lp dichroic (Chroma Technology Corp. Bellows Falls, VT.), or equivalent.
4. Plain microscope slides (Thermo Scientific, Waltham, MA) and No. 1.5 coverslips (Corning, Corning, NY).

3 Methods

Carry out all procedures at room temperature unless otherwise specified.

3.1 Design of Fusion RNA Nanoparticles

1. Use an ultra-stable pRNA-3WJ motif (Fig. 1a, b) as core scaffold to construct fusion RNA nanoparticles. The pRNA-3WJ scaffold can protect RNA from degradation in vivo (*see* **Note 1**).
2. Incorporate sequences of RNA functionalities, such as MG aptamer or Spinach aptamer, at the fusion sites for real time monitoring of RNA folding in vivo (Fig. 1c, 2a, 2b).

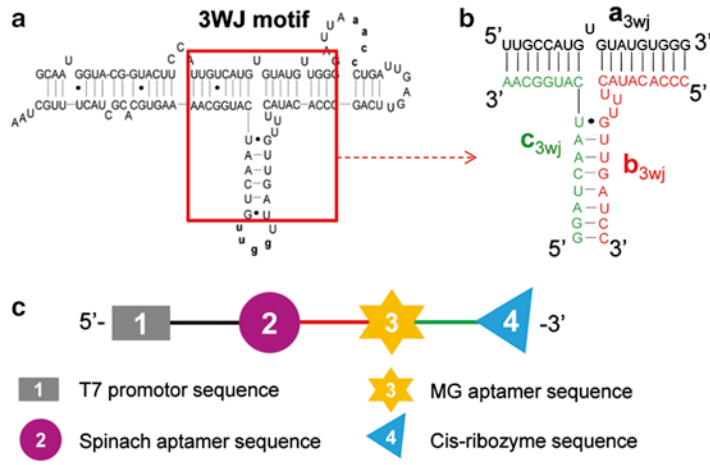

Fig. 1 Design of fusion RNA nanoparticles carrying fluorogenic RNA modules. (**a**) Secondary structure of bacteriophage phi29 motor pRNA. (**b**) pRNA-3WJ motif as a stable scaffold for RNA nanoparticle production. (**c**) Construction of fusion RNA nanoparticles carrying a MG and/or Spinach aptamer sequence for in vitro transcription production, or along with a *cis*-ribozyme sequence for in vivo expression. Figure is adapted with permission from ref. [13] © Oxford University Press

3. For in vitro transcription, add T7 promoter sequence to the 5′ terminus (Fig. 1c) (*see* **Note 2**).
4. For in vivo expression RNA nanoparticles in *E. coli* cells, the lac operon-T7 promoter is used (*see* **Note 3**). A DNA sequence corresponding to *cis*-ribozyme is added at the 3′-end to cleave the undesired sequences arising from uncontrolled termination of transcription during in vivo expression (Fig. 1c) [25]. The DNA template is inserted between BglII/NdeI sites in pET-3b vector to construct the recombinant plasmid.
5. Verify the secondary structures by RNA folding programs, such as M-fold [26].

3.2 Preparation of RNA Nanoparticles by In Vitro Transcription with T7 RNA Polymerase and Purification of the RNA Product with Denaturing Polyacrylamide Gel Electrophoresis

1. Prepare the DNA template based on the sequence design in Subheading 3.1, **steps 1–3** using Polymerase chain reaction (PCR) with GoTaq Flexi DNA polymerase according to the manufacturer's instructions.
2. Assemble a mixture of 10–20 ng DNA template, 1× transcription buffer, 5 mM rNTP solution, 10 mM DTT, and 10–20 % (vol/vol) units T7 RNA polymerase. Mix well and incubate the reaction at 37 °C for 4 h (*see* **Note 4**).
3. Add 1 unit RNase-free DNase I to the reaction and incubate at 37 °C for another 15–30 min.
4. Add one volume of 2× denaturing loading buffer to the reaction and load the sample on an 8 % (wt/vol) urea–polyacrylamide gel. Add an RNA or DNA ladder as size standard in one lane

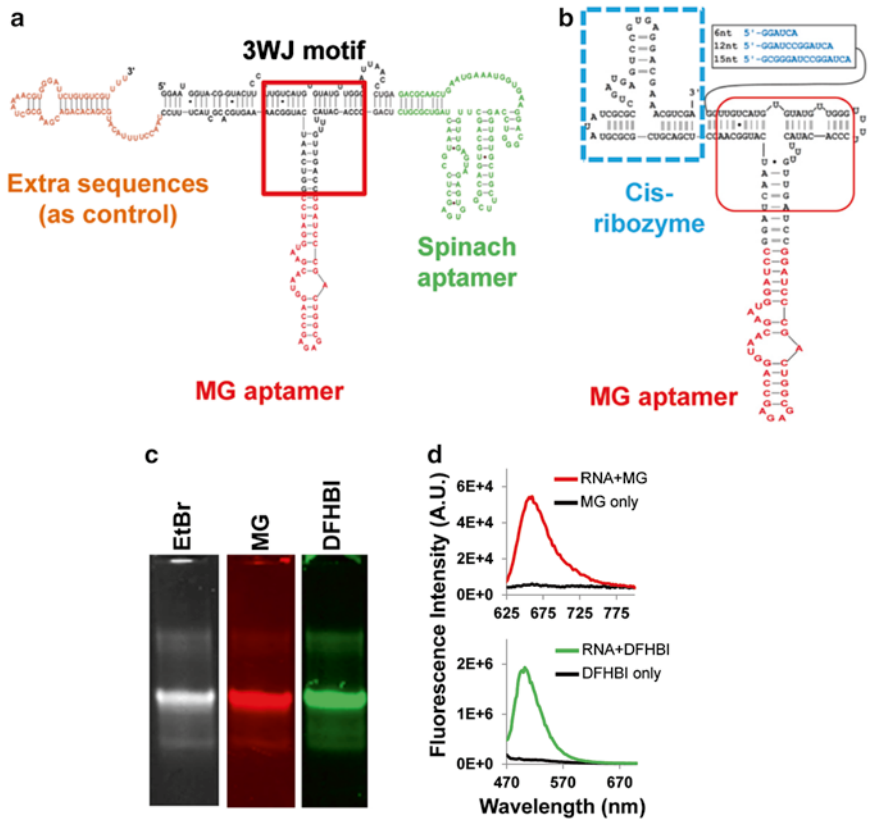

Fig. 2 In vitro assessment of RNA nanoparticles. (**a**) Construct of RNA nanoparticles carrying both MG and Spinach aptamers. (**b**) Another construct of RNA nanoparticles carrying MG aptamer and *cis*-ribozyme for in vivo expression from bacteria cells. (**c**) Assessment of RNA construct in (**a**) by 8 % native polyacrylamide gel. Gel image was taken in different channels after staining with MG, DFHBI and EtBr, respectively. (**d**) Assessment of RNA construct in (**a**) by fluorescence spectra of the RNAs after mixing with different dyes. Figure is adapted with permission from ref. [13] © Oxford University Press

of the gel to facilitate assignment of the correctly sized product bands. Run the gel at RT in 1× TBE buffer at 10 V/ cm (*see* **Note 5**).

5. Detach the gel from the gel plates and shadow the nucleic acid on a TLC plate with a short wave UV lamp (254 nm). Excise the RNA band and mince the gel. Add elution buffer to cover the gel pieces and incubate at 37 °C for 2 h. Collect the supernatant and repeat once for another 2 h (*see* **Note 6**).
6. Combine the supernatants, add 1/10 volume of 3 M sodium acetate at pH 6.5, and 2.5 volumes of 100 % ethanol. Precipitate overnight at −20 °C. Centrifuge the mixture at 16,500×*g* for 30 min at 4 °C. Remove the supernatant and wash the pellet with ice cold 70 % (vol/vol) ethanol. Dry the pellet in a SpeedVac.
7. Resuspend the pellet in 50 μL DEPC-treated water. Determine RNA concentration by OD_{260} (1 OD_{260} = 40 ng/μL).

3.3 Expression, Assembly, and Purification of RNA Nanoparticle Using Bacteria Cells

1. Amplify the DNA fragment based on the sequence design in Subheading 3.1, **steps 1–4** using Polymerase chain reaction (PCR) with GoTaq Flexi DNA polymerase according to the manufacturer's instructions.
2. Purify the insertion DNA fragment by 2 % agarose gel electrophoresis. Recover the DNA band using the QIAEXII gel extraction kit following the manufacturer's instructions.
3. Mix ~15 μg of vector or ~4 μg of DNA fragment with 2 units of BglII, 2 units NdeI, and 10 % (vol/vol) 10× Fast digest buffer. Incubate the reactions at 37 °C overnight. Perform this step separately for both the insertion DNA fragment and the vector (*see* **Note 7**).
4. Purify the DNA fragment after endonuclease cleavage by 1 % agarose gel electrophoresis using the QIAEXII gel extraction kit. Purify the vector after cleavage by 1 % agarose gel electrophoresis and recover the vector with AxyPrep™ DNA gel extraction kit according to the manufacturer's instructions.
5. Set up a 20 μL ligation by mixing ~10 ng of insertion DNA fragment, ~200 ng of vector, 5 units of T4 DNA ligase, 2 μL 10× T4 DNA ligase buffer, and make up to 20 μL with DEPC water. Incubate the reaction at 16 °C overnight (*see* **Note 8**).
6. Verify the sequences of the resulting recombinant plasmids by DNA sequencing.
7. Transform the recombinant plasmid to competent *E. coli* BL21 star cells in KCM buffer using the heat shock method (*see* **Note 9**). Set up the transformation reaction by adding 20 μL ligated recombinant plasmid, 20 μL 5× KCM buffer, and 60 μL Milli-Q water to 100 μL of competent cells. Gently mix, then incubate the cells on ice for 30 min, heat shock at 42 °C for 50 s, and 0 °C for 2 min. Add 800 μL LB medium to the cells and leave to recover at 37 °C for 1 h. Plate cells on LB plates containing 1 % ampicillin and culture at 37 °C overnight. Inoculate the colony into 5 mL LB medium containing 100 μg/mL ampicillin. Culture the cells at 37 °C while shaking at 250 rpm until OD_{600} reaches 0.5. Add 2.5 μL of 1 M IPTG to the cell culture and allow the cells to grow for another 1.5 h.
8. Precipitate the cells by centrifugation using JA-20 rotor at 1,960 × *g* for 20 min at 4 °C and resuspend the pelleted cells in 250 μL Tris–HCl–Mg buffer.
9. Extract the total RNA by adding 500 μL water saturated phenol (pH 4.5) to the resuspended cells. Gently agitate for 1 h at RT and spin the cell debris down at 15,800 × *g* for 15 min at 4 °C (*see* **Note 10**).

10. Transfer the aqueous phase into a new tube and precipitate the RNA following Subheading 3.2, **step 6**. Resuspend the RNA in 50 μL DEPC-treated water.
11. Further purify the desired RNA from total RNA by 8 % (wt/vol) urea–polyacrylamide gel electrophoresis following Subheading 3.2, **steps 4–7**.

3.4 In Vitro Assessment of RNA Folding by Native Polyacrylamide Gel Electrophoresis

1. Load ~200 ng purified RNA nanoparticles from either in vitro transcription or in vivo expression in 1× native gel loading buffer on 8 % native polyacrylamide gel.
2. Run the gel at 4 °C in 1× TBM buffer at 7 V/cm (*see* **Note 11**).
3. Detach the gel from the gel plates and stain with 5–10 μM MG dyes in 1× binding buffer at RT for ~15 min. Scan the gel using Typhoon FLA 7000 gel imager on the Cy5 channel (Excitation at 635 nm/Emission at 670 nm) (Fig. 2c) (*see* **Note 12**).
4. Soak the same gel in water for ~10 min and stain with 2 μM DFHBI dyes in 1× binding buffer for ~15 min. Image the gel on the Cy2 channel (Excitation at 473 nm/Emission at 520 nm) (Fig. 2c) (*see* **Note 12**).
5. Stain the same gel in EtBr for comparison of the sizes with DNA markers. Image the gel on the EtBr channel (Excitation at 532 nm/Emission at 580 nm) (Fig. 2c) (*see* **Note 13**).
6. Overlap all three images to show colocalization of aptamers and RNA nanoparticle (*see* **Note 14**).

3.5 In Vitro Assessment of RNA Folding by MG Binding Assay

1. Prepare a sample of 100 nM RNA nanoparticles with 2 μM MG in 1× binding buffer. Prepare a control sample of 2 μM MG in 1× binding buffer. Incubate at RT in the dark for 30 min (*see* **Note 15**).
2. Record the fluorescence spectra on a spectrofluorometer. Excite MG at 615 nm and scan the emission spectrum from 625 to 800 nm (*see* **Note 16**).
3. Compare the emission spectra to determine the aptamer binding efficiency (Fig. 2d) (*see* **Note 17**).

3.6 In Vitro Assessment of RNA Folding by DHBFI Binding Assay

1. Prepare a sample of 200 nM RNA nanoparticles with 2 μM DFBHI in 1× binding buffer. Prepare a control sample of 2 μM DFBHI in 1× binding buffer. Incubate at RT in dark for 30 min (*see* **Note 15**).
2. Record the fluorescence spectra on a spectrofluorometer. Excite DFBHI at 450 nm and scan the emission spectrum from 470 to 750 nm (*see* **Note 16**).
3. Compare the emission spectra to determine the aptamer binding efficiency (Fig. 2d) (*see* **Note 17**).

3.7 In Vitro Monitoring of RNA Degradation

1. Prepare 1× binding buffers containing the following components: (a) KB cell lysate, (b) RPMI1640 cell culture medium, (c) KB cell culture medium.
2. Incubate 100 nM RNA nanoparticles in 500 μL 1× binding buffer and buffers prepared in step 1 at 37 °C. Take 50 μL from each solution at various time points over the course of 8–10 h. Add MG dye to the solution to 4 μM. Incubate at RT for 10 min (*see* **Note 12**).
3. Record the fluorescence spectra following Subheading 3.5, **step 2**.
4. Compare the emission intensities at 650 nm (maximum emission) over time (*see* **Note 18**).

3.8 Assessment of RNA Folding in Bacteria Cells

1. Take 1 mL of *E. coli* cells from Subheading 3.3, **step 8** and spin down in an Eppendorf tube at 15 × *g* for 3 min at RT.
2. Remove supernatant and resuspend the cells in 1× binding buffer containing 10 μM MG for MG aptamer binding or 10 μM DFHBI for Spinach aptamer binding. Incubate the cells at RT in the dark for ~30 min (*see* **Note 12**).
3. Place ~10 μL of stained cells onto a microscope slide and cover with a coverslip. Transfer the slide to an inverted Olympus IX-71 epi-fluorescence microscope with a 20× objective.
4. Locate a region with a single layer of well spread out cells and take a bright-field image using the halogen lamp on the microscope. Take a fluorescence image of the same region by switching to the Xenon arc lamp and a suitable filter set (*see* **Note 19**).
5. Compare bright-field and fluorescence images to observe MG or DFHBI binding (*see* **Note 20**).

3.9 Assessment of RNA Folding in Eukaryotic Cells

1. Trypsinize KB cells from culture flasks and resuspend to 2.0–5.0 × 10^6 cells/mL in PBS-Mg buffer.
2. Mix 200 μL resuspended cells with 5 μM RNA nanoparticles in a 0.4 cm wide gene pulser electroporation cuvette. Apply a single pulse of 1 kV at 25 μF capacitance using a Bio-Rad Gene-pulser system.
3. Add RNase to the cells to a final concentration of 1 mg/mL, incubate for 10 min at RT. Rinse three times with PBS buffer (*see* **Note 21**).
4. Dilute the cell suspensions in RPMI1640 medium with 10 % FBS to a final concentration of 1.0 × 10^5 cells/mL and incubate at 37 °C.
5. Take 50 μL of cells at various time points over the course of 8–10 h. Centrifuge the cells and resuspend in 50 μL of 1× binding buffer containing 10 μM MG. Incubate the mixture for 30 min (*see* **Note 12**).

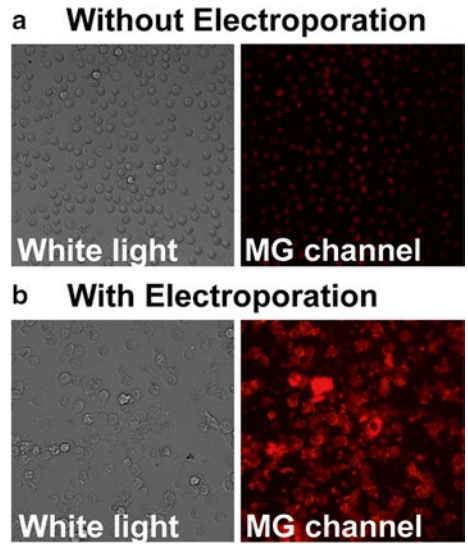

Fig. 3 Epi-fluorescence images of the RNA nanoparticles carrying MG aptamer (**a**) without electroporation and (**b**) after electroporation into KB cells. Figure is reproduced with permission from ref. [18] © Mary Ann Liebert, Inc.

6. Place 20 μL of stained cells onto a microscope slide, cover with a coverslip, and transfer the cells to an inverted Olympus IX-71 microscope with 20× objective.
7. Locate a single layer of well spread out cells and take a bright-field image using the halogen lamp on the microscope. Take a fluorescence image of the same region by switching to the Xenon arc lamp and a suitable filter set (Fig. 3) (*see* **Note 19**).
8. Compare bright-field and fluorescence images to determine MG or DFHBI binding (*see* **Note 20**).
9. Compare images of samples prepared with and without electroporation to determine nanoparticle uptake (Fig. 3a, b) (*see* **Note 22**).

3.10 Determination of the RNA Nanoparticle Half-Life in Real-Time in Animal and Human Cells

1. Prepare cells according to Subheading 3.9, **steps 1–5**.
2. Record fluorescence emission spectra at various time points over the course of 8–10 h as outlined in Subheading 3.5, **step 2**.
3. Compare the emission intensities at 650 nm (maximum emission) versus time.
4. Repeat the time series at least three times. Determine average intensities and standard deviations for each time point and graph versus time (Fig. 4a, b).
5. Fit the graph of average fluorescence intensities versus time using linear regression ($y = mx + t$). Estimate $If_{(1/2)}$, the fluorescence

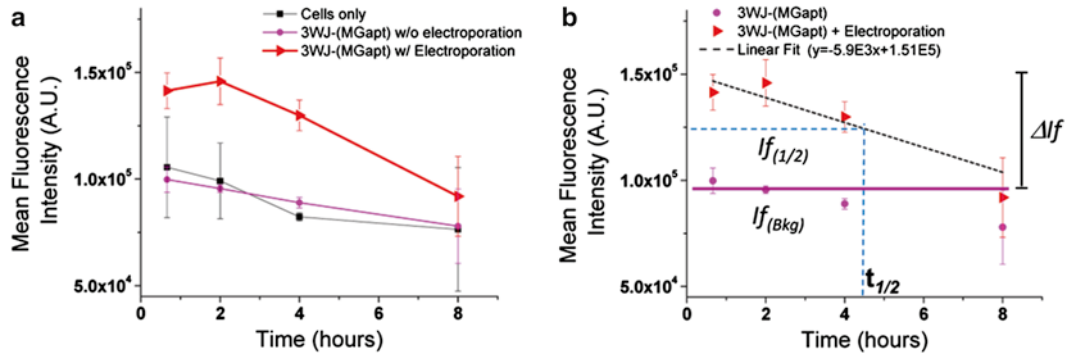

Fig. 4 In vivo assessment of the lifetime of RNA nanoparticles in KB cells. (**a**) Plot shows the changes in fluorescence intensity of the RNAs @ 650 nm over time. (**b**) Calculation of the half-life of RNA after electroporation into the KB cells. Figure is reproduced with permission from ref. [18] © Mary Ann Liebert, Inc.

intensity after half of the RNA has degraded, using Eq. 1: (*see* **Note 23**)

$$If_{(1/2)} = If_{(0)} - \left(\frac{If_{(0)} - If_{(\mathrm{bkg})}}{2} \right) \quad (1)$$

$If_{(0)}$ represents the fluorescence intensity at $t_{(0)}$ (y-intercept of the linear regression) and $If_{(\mathrm{bkg})}$ represents the initial fluorescence intensity of the negative control sample.

6. Estimate the half-life ($t_{(1/2)}$) of RNA nanoparticles in KB cell cultures by substituting $If_{(1/2)}$ in the linear regression, in which $y = If_{(1/2)}$ and $x = t_{(1/2)}$ (Fig. 4b) (*see* **Note 24**).

4 Notes

1. The pRNA-3WJ scaffold is used for in vivo expression of RNA nanoparticles, since it provides protection of the RNA product from degradation by RNases. Most RNases found in vivo attack terminal single strands at either the 5′- or the 3′-end of the RNA. The pRNA-3WJ scaffold provides a compact double strand on both ends to enhance the lifetime of RNA in vivo.
2. The RNA nanoparticles are designed for in vitro transcription with T7 RNA polymerase; therefore, a T7 promoter sequence at its 5′end is necessary. Adding two Guanosine nucleotides to the DNA template sequence immediately following the T7 promoter typically enhances the RNA transcription efficiency. DNA templates typically have the following 5′ to 3′ sequence composition: (a) T7 promoter, (b) Module 1, (c) a_{3WJ}, (d) Module 2, (e) b_{3WJ}, (f) Module 3, (g) c_{3WJ}.

3. The lac-operon-T7 promoter is used for RNA in vivo expression, since it can be regulated and has a high transcription efficiency. This is a great advantage when the RNA product is toxic to the host and prevents the host from growing. It reduces the toxicity foreign RNA causes to the host. The DNA template sequence encoding pRNA nanoparticles is typically designed as follows (a) BglII, (b) T7 promoter, (c) in vitro RNA nanoparticle sequence, (d) *cis*-ribozyme, (e) NdeI.
4. The reaction can be scaled up or down by linearly increasing the volume of each component, while keeping the reaction concentrations constant.
5. To completely denature RNA nanoparticles, heat the RNA solution in denaturing loading dye to 80 °C for ~3 min and snap cool on ice. The migration of loading dyes can be used to monitor RNA migration during the gel run to prevent the RNA from running off the gel. In a 8 % denaturing PAGE gel, location of Bromophenol blue indicates the electrophoretic mobility of a strand of ~20 nt, while Xylene cyanol travels at ~75 nt.
6. To improve the yield of RNA recovery from gel extractions, the first elution can be extended to 5–6 h. Typically, 80–90 % of the RNA elute during the first 3 h.
7. Presence of impurities, e.g., salts, in the restriction digestion lowers the efficiency of DNA cleavage. Hence, it is important to purify DNA fragments and vectors prior to use. Purification in agarose gels with QIAEXII gel extraction kit has worked well for us.
8. The pET-3b vector system works well with a 1:1 molar ratio of DNA insert to vector. However, ratios of 3:1 to 1:3 typically provide good initial parameters. The pET-3b vector is approximately 4 kbp; to calculate the appropriate amount of DNA fragment in the ligation reaction, use the following equation:

$$\frac{\text{amount of vector}\,[\text{ng}] \times \text{size of insert}\,[\text{kb}]}{\text{size of the vector}\,[\text{kb}]} \times \text{molar ratio of insert to vector} = \text{amount of insert}\,[\text{ng}]$$

9. *E. Coli* BL21 star™ (DE3) cells are chosen as host for RNA expression, since the RNaseE gene (*rne131*) in DE3 is mutated to enhance RNA stability. Regular cells with complete RNase activity are likely to yield reduced RNA production efficiency. Handle cells gently to protect from cell lysis. Avoid excessive pipetting as competent cells are very fragile.
10. Phenol is toxic and corrosive, so wear gloves and handle the samples in a fume hood.
11. Native gels containing magnesium should only be run in a cold room and at reduced voltage to protect the RNA from thermal and magnesium-induced degradation.

12. Fluorescent dyes such as MG and DFHBI may photobleach when exposed to light. Always protect the samples from light when using MG and DFBHI dyes for staining.
13. EtBr intercalates into double-stranded DNA and is highly toxic. Make sure to handle ethidium bromide (EtBr) with extreme caution and follow Biosafety regulations.
14. Gels imaged on separate channels can exhibit slight shifts due to differences in the optical alignment across imaging channels. If images from separate channels are to be overlapped in an image processing routine (e.g., ImageJ) to observe colocalization of RNA and fluorogenic modules, the images need to be aligned onto common features in all channels (e.g., gel plate edges are often observable across different channels) to prevent misinterpreting shifts between channels as gel band shifts.
15. Take great care to ensure that both samples are prepared and treated identically to provide a fair comparison of the fluorescence emissions of dyes with and without RNA binding.
16. Based on the chosen emission slit width (i.e., bandwidth of detection) the low wavelength edge of the spectrum might show the falling edge of an intense peak that can at times be much larger than the observed fluorescence peak. This peak is the scattering from the excitation wavelength and can be disregarded as such. If saturation of the detector is observed, start detection at slightly larger wavelengths.
17. To show the increase in intensity from binding of the dyes to the fluorogenic aptamers, the spectra are overlapped for comparison. Great caution has to be taken to record all fluorescence spectra at identical parameters. To allow for true comparison of sample and control, the spectra have to be recorded at the same concentration of dyes (with and without RNA), buffer composition, excitation wavelength and slit width, scan rate, and emission range and slit width. Deviations in any one of these parameters lead to changes in fluorescence intensities.
18. As discussed in **Note 17**, all spectra have to be recorded at identical instrument parameters. At times, the maximum of the emission (center wavelength of the fluorescence peak) can shift with increasing or decreasing overall intensities. In these cases it might be necessary to integrate over the emission spectrum to compare the overall emission intensities instead.
19. The slides should be imaged immediately after preparation as unfixed cells tend to die quickly.
20. A comparison of fluorescence and bright-field images will allow localization of fluorogenic RNA nanoparticles inside the cells. Additional fluorescent labeling of cell organelles is often performed to highlight specific localization.

21. The RNase will degrade RNA nanoparticles that were not taken up into the cell. This step is performed to reduce the fluorescence background in the images. If problems are encountered with intensities in the fluorescence images, this step can be skipped to test whether the problem lies in the nanoparticle concentration or electroporation.
22. Comparison of fluorescence images with and without electroporation (Subheading 3.9, **step 2**), allows determination of RNA nanoparticles bound to the cell membrane versus nanoparticles taken up into the cells.
23. This procedure does not follow a kinetic model. Rather, the linear relation of *If* versus time was observed experimentally and thus employed to estimate $If_{(0)}$.
24. As described above, the half-life is estimated based on the experimental observation of a linear decrease of the fluorescence intensity using the linear regression from Subheading 3.10, **step 5** by substituting $If_{(1/2)}$ back into the linear regression.

Acknowledgement

The research was supported by NIH grants R01EB003730, R01EB019036, and U01CA151648 to Guo P. Guo P is a cofounder of Kylin Therapeutics, Inc., and Biomotor and Nucleic Acid Nanotechnology Development Corp., Ltd. Guo's Endowed Chair of Nanobiotechnology position is supported by the William Farish Endowment Fund.

References

1. Guo P (2010) The emerging field of RNA nanotechnology. Nat Nanotechnol 5:833–842
2. Shukla GC, Haque F, Tor Y et al (2011) A boost for the emerging field of RNA nanotechnology. ACS Nano 5:3405–3418
3. Guo P, Haque F, Hallahan B et al (2012) Uniqueness, advantages, challenges, solutions, and perspectives in therapeutics applying RNA nanotechnology. Nucleic Acid Ther 22:226–245
4. Guo P, Haque F (eds) (2014) RNA nanotechnology and therapeutics. CRC Press, Boca Raton, FL
5. Shu Y, Pi F, Sharma A et al (2014) Stable RNA nanoparticles as potential new generation drugs for cancer therapy. Adv Drug Deliv Rev 66C:74–89
6. Leontis N, Sweeney B, Haque F et al (2013) Conference scene: advances in RNA nanotechnology promise to transform medicine. Nanomedicine 8(7):1051–1054
7. Taft RJ, Pang KC, Mercer TR et al (2010) Non-coding RNAs: regulators of disease. J Pathol 220:126–139
8. Duchaine TF, Slack FJ (2009) RNA interference and micro-RNA-oriented therapy in cancer: rationales, promises, and challenges. Curr Oncol 16:265–270
9. Cayrol B, Nogues C, Dawid A et al (2009) A nanostructure made of a bacterial noncoding RNA. J Am Chem Soc 131: 17270–17276
10. Mattick JS (2009) The genetic signatures of noncoding RNAs. PLoS Genet 5:e1000459
11. Shu D, Shu Y, Haque F et al (2011) Thermodynamically stable RNA three-way junctions for constructing multifuntional nanoparticles for delivery of therapeutics. Nat Nanotechnol 6:658–667
12. Shu Y, Haque F, Shu D et al (2013) Fabrication of 14 different RNA nanoparticles for specific

tumor targeting without accumulation in normal organs. RNA 19:766–777

13. Shu D, Khisamutdinov EF, Zhang L et al (2013) Programmable folding of fusion RNA complex driven by the 3WJ motif of phi29 motor pRNA. Nucleic Acids Res 42:e10
14. Grate D, Wilson C (1999) Laser-mediated, site-specific inactivation of RNA transcripts. Proc Natl Acad Sci U S A 96:6131–6136
15. Paige JS, Wu KY, Jaffrey SR (2011) RNA mimics of green fluorescent protein. Science 333:642–646
16. Afonin KA, Bindewald E, Yaghoubian AJ et al (2010) In vitro assembly of cubic RNA-based scaffolds designed in silico. Nat Nanotechnol 5:676–682
17. Haque F, Shu D, Shu Y et al (2012) Ultrastable synergistic tetravalent RNA nanoparticles for targeting to cancers. Nano Today 7:245–257
18. Reif R, Haque F, Guo P (2013) Fluorogenic RNA nanoparticles for monitoring RNA folding and degradation in real time in living cells. Nucleic Acid Ther 22(6):428–437
19. Paige JS, Nguyen-Duc T, Song W et al (2012) Fluorescence imaging of cellular metabolites with RNA. Science 335:1194
20. Strackharn M, Stahl SW, Puchner EM et al (2012) Functional assembly of aptamer binding sites by single-molecule cut-and-paste. Nano Lett 12:2425–2428
21. Höfer K, Langejürgen LV, Jäschke A (2013) Universal aptamer-based real-time monitoring of enzymatic RNA synthesis. J Am Chem Soc 135:13692–13694
22. Kellenberger CA, Wilson SC, Sales-Lee J et al (2013) RNA-based fluorescent biosensors for live cell imaging of second messengers cyclic di-GMP and cyclic AMP-GMP. J Am Chem Soc 135:4906–4909
23. Kim J, Khetarpal I, Sen S et al. (2014) Synthetic circuit for exact adaptation and fold-change detection. Nucleic Acids Res 42:6078–6089.
24. Chapman EG, Moon SL, Wilusz J et al. (2014) RNA structures that resist degradation by Xrn1 produce a pathogenic Dengue virus RNA. Elife 3:e01892.
25. Hoeprich S, Zhou Q, Guo S et al (2003) Bacterial virus phi29 pRNA as a hammerhead ribozyme escort to destroy hepatitis B virus. Gene Ther 10:1258–1267
26. Zuker M (2003) Mfold web server for nucleic acid folding and hybridization prediction. Nucleic Acids Res 31:3406–3415